Geology, Alteration, and Metal Distribution of the Buffalo Valley Gold Deposit, Battle Mountain, Nevada

by

Kathryn Sechrist

A Prepublication Manuscript Submitted to the Faculty of the

DEPARTMENT OF GEOSCIENCES

In Partial Fulfillment of the Requirements
for the Degree of

MASTER OF SCIENCE

In the Graduate College
THE UNIVERSITY OF ARIZONA
2012

STATEMENT BY THE AUTHOR

This manuscript, prepared for publication in the has been submitted in partial fulfillment of requirements for the Master of Science degree at The University of Arizona and is deposited in the Antevs Reading Room to be made available to borrowers, as are copies of regular theses and dissertations.

Brief quotations from this manuscript are allowable without special permission, provided that accurate acknowledgment of the source is made. Requests for permission for extended quotation from or reproduction of this manuscript in whole or in part may be granted by the Department of Geosciences when the proposed use of the material is in the interests of scholarship. In all other instances, however, permission must be obtained from the author.

(author's signature) *(date)*

APPROVAL BY RESEARCH COMMITTEE

As members of the Research Committee, we recommend that this prepublication manuscript be accepted as fulfilling the research requirement for the degree of Master of Science.

Major Advisor *(Spencer Titley)* *(signature)* *(date)*

(Mark Barton) *(signature)* *(date)*

(Eric Seedorff) *(signature)* *(date)*

Table of Contents

Abstract

This study presents new data on the Buffalo Valley deposit, which is one of many mid-Tertiary gold-(copper) deposits in northern Nevada that contains porphyry dikes fringed by skarn. Not far from the deposit there are a number of copper-poor Carlin-type deposits without skarn. The Buffalo Valley gold deposit lies in low hills on the eastern side of Buffalo Valley and on west-central edge of Battle Mountain. The Buffalo Valley, Phoenix (Copper Canyon, Fortitude), and Converse deposits are among the porphyry-related skarn deposits in the greater Battle Mountain area that are related to intrusions. Buffalo Valley historically produced ~50k oz (~1500 kg) of Au and is being prepared to again go into production with a reserve containing ~ 600k oz (~20,000 kg) of Au.

Several generations of Eocene to Oligocene granodioritic to dacitic porphyry dikes intrude clastic, calcareous, and basaltic rocks of the late Paleozoic Havallah sequence. The porphyry dikes and mineralized system are truncated on the western side by a post-ore normal fault that dips ~40ºW, and the attitudes of post-ore strata indicate that the system has been tilted ~25ºE. Dikes range in SiO2 content from 61.90 to 69.40 %. Alteration at Buffalo Valley is strongly influenced by host rock lithology and proximity to specific dikes and includes siliceous, biotite and calc-silicate hornfels, and skarn within the Havallah sequence and potassic, sericitic and calcic within the igneous dikes. Compositions of garnets and pyroxenes in skarn fall within the andradite and diopside-salite range respectively, and sodic-calcic alteration contains plagioclase and actinolite. Gold principally occurs as free gold within oxidized pyrite and arsenopyrite deposited during quartz+sericite+pyrite alteration. Within pervasively clay altered dikes pyrite can contain up to 10.8 raw weight % As.

The pattern of metal distribution is neither simple nor symmetrical because of variable lithology and structural dismemberment and tilting, but Pb+Zn±Ag±Hg generally are peripheral to a core of Au+Cu±Ag±Hg. Zonation patterns at Buffalo Valley are broadly similar to other porphyry-related systems.

Introduction

Northern Nevada is a major gold province and contains a variety of deposit types, many of which formed in the late Eocene and early Oligocene, and one of the better mineralized areas is at Battle Mountain. Battle Mountain contains other Eocene-Oligocene gold-copper deposits, including Phoenix (Copper Canyon, Fortitude) at the southern end of the range, Converse-Redline at the head of Buffalo Valley (Cleveland, 2000), a series of small deposits in the Copper Basin area on the northeastern part of the range (Theodore, 2000; Keeler, 2010), and Upper Paiute Canyon and Elder Creek at northern part of the range (Ivosevic and Theodore, 1996; Theodore, 1996) and additional deposits are located nearby, such as Cove-McCoy (Brooks et al., 1991; Johnston, 2000; Johnston et al.; 2008). North of Buffalo Valley several distal disseminated Au deposits occur including the Lone Tree and Marigold deposits (Braginton, 1996; Bloomstein et al., 2000; McGibbon and Wallace, 2000; Young et al., 2000). In addition, the area contain porphyry molybdenum systems, such as the molybdenum prospects at Buckingham (Blake, 1992; Doebrich, 1995; Keeler and Seedorff, 2007) Buffalo Valley Mo (Thomas, 1985; Doebrich, 1995; Doebrich and Theodore, 1996) and Trenton Canyon (Felder, 2000). These magmatic-hydrothermal deposits formed contemporaneously with other gold deposits in the region, including an adularia-sericite epithermal deposit at Tuscarora and many Carlin type deposits.

Further work on deposits such as Buffalo Valley might shed light on the origin of all of the Eocene-Oligocene deposits in the area. The purpose of this study is to add to the existing knowledge of Buffalo Valley and address details of the alteration not previously considered. This study will also add to the overall dataset for Battle Mountain, hopefully aiding in future exploration and study of the area.

Buffalo Valley has many characteristics that could place the deposit into a porphyry related Au (-Cu) deposit or a distal disseminated Au deposit. The author claims that Buffalo Valley represents a specific transitional niche that combines characteristic (telescoping?) features of both models. A better understanding of such transitional deposits would lead to a better plan of attack for future exploration within northern Nevada where granodioritic to tonalitic magmas occur within close proximity to distal disseminated and Carlin-type deposits.

This thesis begins with a review of the geology within the Battle Mountain mining district and the basic features of the geology at Buffalo Valley. The thesis will focus on the alteration that occurs within the Havallah sequence with special attention paid to the compositions of garnets and pyroxenes within the skarn alteration and compositions of pyrites and arsenopyrites in ore grade samples. Then the geochemistry and metal distribution at Buffalo Valley will be addressed followed by a discussion of the implications for the types of alteration, mineral compositions and metal distributions present, considering how Buffalo Valley fits into a porphyry related Au (-Cu) or a distal disseminated Au deposit.

Location, History, and Previous Work

The Buffalo Valley deposit is located in low hills on the eastern side of Buffalo Valley and on the west-central margin of the subequant mountain range of Battle Mountain, south of the town of Valmy. The Buffalo Valley deposit has been considered part of the Buffalo Valley mining district (e.g., Tingley, 1992), but for the purpose of this study the deposit and mining district are considered part of the greater Battle Mountain district.

The Battle Mountain mining district is located in north-central Nevada southwest of the town of Battle Mountain and Interstate Highway 80. The district is situated approximately 90 km west of the Carlin trend, 60 km south of the Getchell trend, and 65 km northwest of the Cortez district, all host to Carlin-type deposits. (Fig. 1).

Intermittent mining at Buffalo Valley occurred between 1924 and 1951 producing approximately 1,200 oz. Au, 1,380 oz. Ag, and 9,607 lbs. Cu with average grades of 0.41 oz Au/t, 0.47 oz Ag/t, and 0.002% Cu (Roberts and Arnold, 1965; Seedorff et al., 1991). Between 1987 and 1990 Horizon Gold Shares, Inc. operated an open-pit mine and heap leach facility which produced 47,453 oz Au with an approximate grade of 0.040 oz Au/t (Reid et al., 2011).

In 2006 Newmont Mining Corporation entered into a joint venture with Fairmile Gold Mining, Inc.. As of 2009, Newmont has defined approximately 30 million tons with an average grade of 0.021 oz Au/t and containing 630,000 oz of gold. The reader is encouraged to review previous work on Buffalo Valley by Roberts and Arnold (1965), Seedorff et al. (1991), Doebrich (1995), Kizis et al. (1997) and Reid et al. (2011).

Regional Geology

The geologic history of the Battle Mountain mining district is complex and has been well described by many previous workers (Roberts, 1964, Roberts and Arnold, 1965, Stewart, 1977, and Doebrich, 1995). Battle Mountain consists of a set of thrust sheets which include the following; the Roberts Mountains allochthon, the autochthonous Antler Overlap sequence, and the Golconda allochthon. Cretaceous and Tertiary plutonic rocks have intruded the Paleozoic assemblages. Cenozoic ash-flow tuffs and alluvium locally overlie the older rocks, and Cenozoic basalts also occur in the district (Roberts, 1964).

The Roberts Mountain allochthon comprised of quartz arenite, chert and greenstone of the Ordovician Valmy Formation, and chert, shale, argillite and greenstone of the Devonian Scott Canyon Formation (Roberts, 1964) was emplaced above the Roberts Mountains thrust during the late Devonian to early Mississippian Antler orogeny. The feldspathic sandstone of the Cambrian Harmony Formation overlies the Valmy and Scott Canyon Formations which was carried in along the Dewitt thrust, a major splay of the Roberts Mountains thrust (Doebrich, 1995).

Comformably overlying the rocks of the Roberts Mountains allochthon are the autochothonous Pennsylvanian to Permian rocks of the Antler Overlap sequence. The Antler sequence consists of material eroded from the Antler highlands during the Antler orogeny (Roberts, 1964). This sequence consists of conglomerate, sandstone, siltstone and limestone of the middle Pennsylvanian Battle Formation, bioclastic and sandy limestone of the Antler Peak Limestone, and pebble conglomerate, sandstone and siltstone of the Permian Edna Mountain Formation (Roberts, 1964).

The final succession of Paleozoic rocks within the Battle Mountain mining district are those composing the Golconda allochthon. These rocks were emplaced above the Golconda thrust. The Golconda allochthon consists of tectonically interleaved chert, argillite, shale, siltstone, sandstone, conglomerate, limestone and greenstone of the Mississippian to Permian Havallah sequence (Roberts, 1964). For this study the tectono-stratigraphic nomenclature of Murchey (1989, 1990) will be employed.

A large number of stocks and dikes intrude the Paleozoic succession. Most are felsic and calc-alkaline granites and granodiorites (Theodore et al., 1973; Theodore, 2000). Plutons range in age from Cretaceous, at Trenton Canyon (89 Ma) and Buckingham (92-99 Ma), to late Eocene to early Oligocene in the rest of the district (Theodore et al.; McKee, 200; 1973, Keeler, 2010). Various suites of Teritary volcanic rocks crop out in the Battle Mountain mining district and include Oligocene to Miocene tuffs and Oligocene basalts (Theodore, 2000).

Geology of the Buffalo Valley Deposit

The Buffalo Valley deposit is located within a tilted fault block bounded to the east by the Front fault and to the west by the Buffalo Valley fault. The deposit is hosted in the upper portion of the Mississippian – Permian Havallah sequence (lithotectonic unit 2). At Buffalo Valley, the Havallah sequence is intruded by granodiorite dikes of Eocene age (33-37 Ma). Unaltered, tilted Cenozoic ash flow tuffs unconformably overlie the Havallah sequence and intrusive rocks (Fig. 2).

Sedimentary Rocks of the Buffalo Valley Deposit

Havallah sequence

The Havallah sequence has been described and divided a variety of ways (Roberts, 1964, Stewart et al., 1977, 1986; Tomlinson, 1990; Murchey, 1990; Seedorff et al., 1991) (Fig HavNames). For this study the classification of Murchey (1990) will be used.

The Buffalo Valley deposit is hosted within Lithotectonic unit 2 (LU-2) of the Havallah sequence. LU-2 is a basinal sequence of chert, siltstone, sandstone, limestone, turbidites and submarine volcanics (Doebrich, 1995). Several subunits of the LU-2 of the havallah sequence occur at Buffalo Valley. A chert and siltstone subunit consists of thinly bedded to laminated black, green, grey, tan and dark brick red silty chert and calcareous siltstone. Soft sediment deformation features are often preserved. A metabasalt occurs within this chert and siltstone subunit at Buffalo Valley and is exposed in the current pit. For this study, the Newmont practice of separating the basalt (Phgc) from the chert and siltstone (Phc) lithology in the subunit is followed. Along the southeastern wall of the current pit pillow textures are observed in exposed basalt, suggesting that the basalt is a submarine flow of variable thickness (Reid et al. 2010). Also present at Buffalo Valley are limestone subunit consists of interbedded dark grey to black limestone, silty to sandy limestone and chert (Phls) and a light grey, argillaceous siltstone subunit (Pha).

Igneous Rocks of the Buffalo Valley Deposit

In general, igneous rocks at Buffalo Valley are granodioritic in composition. The dikes range in SiO2 content from 61.90 to 69.40% (Table 1). Phenocrysts mostly consist of plagioclase, hornblende and biotite, and constitute between 25-80 vol% of the rock (25-30vol% being the average) (Doebrich, 1995). The groundmass generally consists of quartz and potassium feldspar (Fig 3). Accessory minerals include titanite, magnetite and ilmenite. Primary biotite and hornblende from exposed granodiorite porphyry rocks at Buffalo Valley yielded K-Ar ages of 36.9±1.1 and 33.7±1.1 Ma respectively (McKee, 2000). The reader is encouraged to read Seedorff et al's. (1991) description of igneous rocks at Buffalo Valley. New data from Newmont and this study are described below.

Miscellaneous Igneous Rocks

Narrow porphyry dikes, rare pebble dikes and lamprophyres also occur within the Buffalo Valley deposit, but are not large enough to be mappable. Pebble dikes contain subrounded clasts of Havallah within a green, fine grained igneous matrix and have been observed within the current pit and also within drill holes. Lamprophyre dikes, as defined by Williams, Turner and Gilbert (1982), also occur in the Buffalo Valley mine area. Although these intrusive rocks are heavily altered, petrographic work by McComb (2009) show that these lamprophyres contain microphenocrysts of pale green amphiboles within a distinct felty textured groundmass of plagioclase laths with interstitial quartz and potassium feldspar. A relatively unaltered lamprophyre dike from NBV-00032 at depth (>1900 ft) contains phenocrysts of zoned orthopyroxene (enstatite-ferrosilite whose rims are more Fe-rich than its cores), and olivine within a felty groundmass of plagioclase, colorless amphibole, orthopyroxene (enstatite-ferrosilite) and interstitial potassium feldspar and quartz (McComb, 2009). Within NBX-00261 a very dark, fine grained dike occurs, which is intensely altered (Fig 4). Due to the destruction of the texture, it has been dubbed the "mystery rock." The occurrence of the rock in core and the presence of phenocryst ghosts under the petrographic scope lead the author to believe the rock is in fact igneous. The mystery rock will be revisited in the alteration section.

Cenozoic ash-flow tuffs

Unconformably overlying the Havallah sequence and porphyry intrusions are unaltered, east-dipping interlayered Cenozoic ash-flow tuffs and alluvium. At some locations, these rocks rest directly on altered dacite porphyry dikes with anomalous gold (Seedorff et al., 1991). Tertiary gravels consist of cobbles and boulders of Battle Formation conglomerate and plutonic rocks of an unknown origin. Clasts from the Battle Formation suggest there was an east-west trending drainage system transporting material from the east (Roberts, 1964, Seedorff et al., 1991 and Doebrich, 1995). Ash-flow tuffs occur interleaved within the Tertiary gravels and alluvium as well as draping over the Tertiary paleotopography. Although the tuffs at Buffalo Valley have no radiometric age determinations, lithologically similar tuff from the North Peak Quadrangle and the 8 South pit at the Marigold mine yield K-Ar ages of 25.5±0.8 Ma and 22.9±0.7 Ma (McKee, 2000).

Structure at the Buffalo Valley Deposit

The Havallah sequence suffered deformation during and possibly prior to emplacement along the Golconda thrust. Beds in the Havallah sequence generally strike northwest to north-northeast and dip 40-65° west to southwest. Close to isoclinal folds are exposed within the current pit and in out crop in the surrounding area (Seedorff et al., 1991, Doebrich, 1995, Reid et al., 2010). Wispy textures, resembling soft sediment deformation, are observed and preserved locally in the Havallah. These textures could have formed prior to or contemporaneous with the emplacement of the Havallah. Thrust faults are reported within the Havallah at other localities, and Seedorff et al. (1991) interpret the contact between the base of the basalt and the lower lithologies as a thrust fault.

West dipping Basin and Range normal faults form the eastern (Range fault) and western (Front fault formerly Buffalo Valley fault) boundaries of the Buffalo Valley fault block. The Front fault, generally striking north-south and dipping 35-45°, is mineralized and also offsets unaltered post mineral strata, implying that the fault was active during and after gold deposition at Buffalo Valley (Reid et al., 2011). Emplacement of these normal faults results in roughly 25° of tilting to the east as seen in tilted bedding with the Cenozoic strata (Seedorff et al., 1991). Although no dikes were emplaced in the Tertiary faults at Buffalo Valley, elsewhere in the district these normal faults control dike emplacement. For example the Virgin Fault at Copper Canyon is occupied by an extension of the Copper Canyon stock (Doebrich, 1995).

Alteration and Metal Distribution at Buffalo Valley

Ore at Buffalo Valley is hosted within oxidized, sheeted pyrite veins that cut across all lithologies in the deposit. These ores are concentration of supergene alteration minerals derived from primary ores of a succession of metamorphosed sedimentary and volcanic strata. The alteration of the Havallah group within the fault block is characterized by a major thermal event of unknown origin that converted its fine-grained, clastic strata to hornfels of varied mineralogical composition, but with little or no change in bulk chemical composition, its distinctive calcareous units to marble and skarn assemblages, and was overprinted by the effects of hydrothermal activity and fracturing associated with igneous intrusions. There may well be only two events of significance that resulted in redistribution of elements of the host, and later introduction of metals by igneous activity. The discussion of alteration will occur in two parts: The first section will be a review of the alteration that occurs with the various lithologies of the Havallah sequence, and the second section will be a review of the alteration that occurs within the intrusive rocks.

Alteration within the Havallah sequence

Lithology has a strong control on alteration within the Havallah sequence at Buffalo Valley. The overall fine grained nature of the host rock is such that metasomatism is confined to the few occurrences of coarser grained sand and limestone, fractured or brecciated material, and in veins.

Fine grained sandstone and argillite are commonly altered to light to dark grey hornfels, with little or no change in bulk composition. In slightly coarser examples of this material carbonate, wollastonite and minor amounts of diopside-salite will occur around grain boundaries. Siltstones and shales are altered to a dark red brown or pinkish tan biotite hornfels. The calcareous strata at Buffalo Valley are altered to a medium to dark olive green diopside-salite hornfels (Fig 5). Medium to coarse grained sandstone often contains interstitial sericite and carbonate. The coarser grained sandstones also contain pods of wollastonite and either diopside-salite or actinolite.

Rare skarn alteration occurs within limestone. Two distinct assemblages have been determined thus far. The first skarn assemblage (skarn1) contains andradite+diopside-salite+pyrite+chalcopyrite+pyrrhotite. The sulfides are disseminated and also occur in veins.

A Ag-Te mineral occurs within a chalcopyrite grain in the skarn1 assemblage. Skarn1 contains very trace amounts of native Ag. The second skarn assemblage (skarn2) contains wollastonite+diopside-salite+andratite-grossular+pyrrhotite+galena+sphalerite. Again, the sulfides are disseminated or occur in veins. In skarn2 the andraditic garnets contain Al-rich (grossularitic cores) and in some instances albite occurs within the garnet core. Apatite occurs in both skarn assemblages.

Microprobe analyses show that garnets and pyroxenes are compositionally zoned (fig 6). Garnets in skarn1 have Mg-rich cores, Fe-rich rims and generally fall within the andradite range (fig. 7 and table 2). Garnets within skarn2 have Al-rich cores and fall closer to the grossular range (fig. 7). Pyroxenes have Fe-rich rims and generally Mn and Al increase from core to rim. Pyroxene compositions fall within the diopside-salite range (fig. 8 and table 3).

Alteration within the intrusive rocks

Several different alteration types occur within the intrusive rocks at Buffalo Valley. Skarn (endoskarn) alteration occurs mostly within the porphyry dikes west of the current pit. The endoskarn alteration consists of an assemblage of secondary actinolite with varying amounts of quartz, plagioclase and pyroxene. In some instances pyroxene has been observed replacing hornblende (McComb, 2009). Associated with this assemblage are multiple generations of quartz veins and veinlets of pyroxene. Fine grained pyrite and chalcopyrite occur in this assemblage and are disseminated or within quartz veins. Molybdenite only occurs within quartz veins.

Potassic alteration consists of an assemblage of secondary minerals of quartz+biotite+k-feldspar with pyrite, chalcopyrite and molybdenite. This alteration occurs within Tpg2 which cuts the chlorite and sulfide bearing assemblage within Tpg1. Amphiboles within potassically altered rocks are replaced by biotite and later by chlorite. Feldspars are mostly intact, but where the grains are fractured fine grained biotite can be found. Sulfide and iron oxides, mostly ilmenite, occur within the groundmass, in veins and also within mafic sites. Veins that occur with potassic alteration include quartz±k-feldspar, quartz+pyrite and quartz+molybdenite+chalcopyrite. All of these vein types have sharp edges with only minor biotite envelopes (fig 9).

Sericitic alteration consists of an assemblage of secondary quartz+sericite+pyrite±arsenopyrite and occurs specifically within the dacite dikes occurring in the eastern and northern parts of the deposit (Seedorff, 1991). In intensely altered samples, felsic and mafic phenocrysts are replaced by sericite and fractures are filled with sericite. Quartz veins are abundant with or without sulfides. FeOxs in vein quartz occur after pyrite and arsenopyrite.

Alteration of Miscellaneous Igneous Rocks

Alteration of the lamprophyres at Buffalo Valley is well described by Newmont geologist Mark McComb. Within skarned lamprophyres, mafic sites are altered to amphiboles and pyroxenes with minor phlogopite. Locally epidote and chlorite replace amphiboles. Potassically altered lamprophyres consist of an assemblage of secondary biotite+quartz+actinolite+pyrite+chalcopyrite+pyrrhotite. Galena and sphalerite are observed rimming the other sulfides. Clay alteration is common and can contain Au concentrations up to

6.6ppm. Clays range from mixed illite-smectite to mixed illite-montmorillinite. Other minerals present include k-feldspar+sericite+Fe-oxides after pyrite and arsenopyrite.

Alteration of the "mystery rock" is pervasive and the original texture is completely obscured. Analysis with the EMP shows that the material is mostly Si and Ca (quartz and carbonate). When assayed the interval in which the dike occurs contained roughly 0.25 opt Au. Within this dark dike fine grained pyrites occur. The pyrites occurring within the dike contain up to 10.3 raw weight % As and trace amounts (up to 0.22 raw weight %) of Sb. The pyrites occurring within the wall rock contain <1 raw weight % As (table 4).

Veins

Cutting across the hornfelsed and skarned material at Buffalo Valley are several different vein types. In both biotite and siliceous hornfels, chlorite+actinolite+chalcopyrite+pyrrhotite occur in veins and also as the matrix in brecciated samples. In general those veins containing calc-silicates are the oldest. The calc-silicate bearing veins are cut by various generations of quartz and quartz+sericite+pyrite (QSP). The quartz veins and QSP veins cross cut each other. Calcite veins are always late, and wide (2-3cm) calcite veins containing coarse sulfide and clasts of host rock appear to be the youngest vein type.

Depth of Weathering

At Buffalo Valley Reid et al. (2011) reports an average depth of oxidation along the structural trend to 244 m (800 ft). Oxidation has been observed up to approximately 670 m (2190 ft) depth in core. Seedorff et al. (1991) describes zones of broken rock up to 10 m wide and with little to no offset that guide locally deep supergene alteration.

Distribution of Metals

Cross sections showing the spatial relationships between host rock lithology, alteration and the concentration of Au, Cu, Ag, Hg, As, Pb, and Zn were constructed based on drill logs and whole rock geochemical analyses. Two cross sections will be examined. Cross section 1 is located at the northern end of the pit, with the eastern margin terminating with the pit. Cross section 2 is located at the southern end of the pit, crosses the entire pit and bends slightly to the northeast.

Looking at cross section 1, one can see that the host rock lithology consists of the "greenstone" or basalt unit of the Havallah sequence, which is cut by a granodiorite dike. Two other granodiorite dike are observed within the cross section but do not cross cut any other igneous rock. Mostly the lithology of this cross section is siltstone with beds of limestone and sandstone. There is a chert unit near the large main intrusion. Alteration within this cross section is varied but a general trend of lithology and the associated alteration type can be established. QSP alteration occurs in and slightly around the intrusive bodies. Siliceous hornfels occurs throughout most of the Havallah sequence. Biotite hornfels occurs as well and there seems to be some spatial association with the intrusions. Calc-silicate hornfels occurs mostly around the limestone units and around the basalt. Skarn alteration also occurs, mostly within the limestone lithologies and also within some of the granodiorite dikes.

Gold (>0.01opt) appears to be slightly controlled by bedding but mostly occurs near the margins of the granodiorite dikes. Mercury (>0.02ppm) is also spatially associated with the intrusions and therefore with higher gold concentrations. Arsenic (>100ppm) is also found near the margins of the dikes and the highest concentrations occur where gold is found in higher concentrations. Increased copper concentrations (> 100ppm) are fairly widespread, mostly in the higher portions of the systems, but still spatially associated with the dikes.

There is no significant Pb (>100ppm) in this part of the system. Zn (>100ppm) is sparse in this part of the system, and is more likely controlled by bedding or lithology since there is little spatial association with the intrusives. Zn does appear to be spatially associated with increased Ag concentration (>1.0 ppm). Ag concentrations correspond with some Au concentrations (below the main intrusive dike) but are also likely more controlled by bedding and lithology. Increases in Ag concentrations occur either within limestone litholgies or below the limestone and sandstone lithologies, again suggesting lithological controls (fig.).

Cross section 2 consists of similar lithologies as cross section 1, with the basalt or "greenstone" unit, two main intrusive dikes and some smaller dikes. There is a limestone bed that occurs in the lower parts of the cross section, and few limestone beds are found in the northwestern portion of the cross section. Cherty lithologies also occur in the lower portion of the cross section and a few cherty beds are found in the northwestern portion of the cross section. QSP and potassic alteration again mostly occurs within the intrusions, but some QSP is reported in the Havallah, especially below the eastern intrusion and also between the two main intrusive bodies. Clay alteration is reported in the lower portion of the main western intrusion. The lower limestone bed is altered to marble and calc-silicate hornfels. Mostly the Havallah is altered to either a siliceous hornfels or a biotite honrfels. A small portion of endoskarn is recorded for a very central part of the eastern main intrusion.

Au concetrations (>0.01opt) are again spatially associated with the intrusions especially east of the main western intrusion. There also appears to be some control by bedding, note especially a pooling effect below the cherty lithology in the northwestern portion of the cross section. Increased mercury (>0.2 ppm) and arsenic values (>100 ppm) correspond well with the increased Au values. Copper values (>100ppm) also correspond with increased Au values, especially in the lower portions of the system, but in the upper portions there is a slight Cu anomly without a corresponding increase in Au. One can see here the higher concentrations of Cu within the basalt unit.

In cross section, one can see the greater control that lithology has on the base metals at Buffalo Valley. In the lower limestone bed one can see higher Pb (>100ppm), Zn (>100) and Ag(>1.0ppm) values. Increases in Ag values also show some correlation with increased Au concetrations, but is also controlled by bedding and lithology. Zn shows a very slight correspondence with Au values, espeacially to the east of the western main intrusion. Zn values are also slightly elevated in the northern portion of the eastern intrusion and in the easternmost cherty lense (fig. 10).

Gold Occurrences

Detailed metallurgical studies by Newmont have helped to characterize the nature of gold of Buffalo Valley. Gold at Buffalo Valley commonly occurs with FeOx and/or sericite (figAu1). Barren pyrite grains can have gold bearing oxidized arsenopyrite rims (figAu1). Gold has also been found with FeOx rimming or occurring within other minerals, most commonly sericite but also k-feldspar, quartz and FeOx within garnets. Gold has also been found to occur within amphiboles and pyroxenes. Fischesserite (Ag_3AuSe_2) has been found locked within sericite. Trace element studies on pyrite and arsenopyrite grains collected from gold rich intervals within drill hole NBV-00261 show two distinct pyrite groups, one that is arsenic rich and one that is not. As-rich pyrites contain Cu and Cr, while As-poor pyrites tend to be more pure in terms of trace elements. Arsenopyrites contain anomalous Sb, Ni and Co (table X). Within the analyzed sulfides Te and Bi are found in very trace amounts, however these elements are present within trace occurrences of silver tellurides or bismuth chlorides.

Discussion

Implications of Skarns

At Buffalo Valley garnets are mostly andraditic and pyroxenes fall within the diopside-salite range. These types of compositions are more like those that occur in porphyry related oxidized Cu skarns (Meinert, 2000). The presence of arsenopyrite is associated more with reduced skarn deposits, and although arsenopyrite is present at Buffalo Valley it is not associated with the skarn alteration (Meinert, 2000). The lack of arsenopyrite within the skarn assemblages could also imply a more oxidized environment during the period of skarn alteration.

The rarity of skarns at Buffalo Valley and their location within specific lithologies suggest that either the skarn producing era did not last long enough to produce a large skarn such as that found at the Phoenix mine. This could also suggest that perhaps Buffalo Valley is too far from the source of fluids and heat. The simplest explanation could just be that the Havallah sequence is too poor of a host rock to support significant gold deposition. Elsewhere within the district the Havallah sequence often acts as a metallotect.

Implication of Metal Distribution

Metal zoning patterns can also be useful in exploration. Typically, a porphyry Cu±Au deposit will contain an ore body in and around the main porphyry stock, a central core of anomalous Cu, Mo, Au and Ag, and a farther reaching halo of anomalous Cu, Pb and Zn (Rose, Hawks and Webb, 1979). These metal patterns can be complicated by various intrusive events and lithology controlled mineralization, but the general patterns can still prove useful to the exploration geologist.

Buffalo Valley has a central area of Au+Hg+As±Cu±Ag, with slightly distal Cu, and distal Zn+Pb±Ag, especially in the southern portions of the mine area. The Fortitude-Copper Canyon area in the south central portion of the Battle Mountain Mining District has a central area of increased Au and Cu, with a halo of Hg around the Au (ref). The halo of Hg around the Au is different from Buffalo Valley, where the Au and Hg anomalies correspond. Fortitude-Copper Canyon also has distal anomalous Pb+Zn. The Elder Creek porphyry prospect, which has low mineralization overall, has a correspondence between Au and As in the southern portion of the area. Elder Creek has Cu anomalies around the central porphyry and distal anomalous Pb+Zn (King, 2011).

At Buffalo Valley, metal distribution is neither simple nor symmetrical, which is a result of a complex host rock lithology and structural history. Increased concentrations of

Au+As+Hg±Cu±Ag occur along the margins of granodioritic porphyry dikes. Zn+Pb±Ag are distal to Au and also occur in altered limestone beds. Metal patterns at Buffalo Valley are broadly similar to those seen at other Cu porphyry deposits.

Classification of Buffalo Valley

Although the author is of the opinion that often times science and geology is too model driven, at the beginning stages of exploration and even up through near mine brownfields exploration a model and classification of a deposit can certainly help to guide exploration and drilling in a successful (diction) direction.

Although Buffalo Valley could be classified as and shows many characteristic features of various deposit types (porphyry, distal disseminated, Au skarn), the author places Buffalo Valley within a unique transitional or hybrid niche. Evidence exists to suggest a deeper porphyry source of heat and fluids yet no large igneous body has been found to date. Others have classified the deposit as a reduced Au skarn (Meinert, 2000), yet BV only has minor occurrences of reaction skarn containing difficult to recover gold. Garnet and pyroxene compositions and the sulfides present suggest a more oxidizing environment for skarn formation. Distal disseminated is another type attributed to BV based on a sedimentary host and geochemical signatures (Cox and Singer, 1986; Cox, 1992; Reid et al., 2011). Au occurrence in QSP+arsenopyrite veins and other alteration types in deposit do suggest that Buffalo Valley occurs at a higher level within a porphyry model and more distal to a larger heat source (Seedorff et al. 1991; King, 2011).

Acknowledgment

I would like to thank Newmont Mining Corporation and the Science Foundation Arizona for the financial support of this project. I would like to thank my advisor, Spencer Titley, for his patience, understanding, and for sharing his immense store of knowledge and experience in geology and mining. I would also like to thank the others on my committee, Mark Barton and Eric Seedorff, for their patience and guidance as well. Thank you to Newmont geologists Richard Reid, Jeff Nichols, and Rendy Keaton for their support in the office, the core shed and the field, and thank you to the core technicians for their work, especially Randy Mullinax, who sadly passed away shortly after my first summer working with Newmont.

References

Cox, D.P., 1992, Descriptive modelfor distal disseminated Ag-Au *in* Bliss, J.D., ed., Developments in Mineral Deposit modeling: U.S. Geological Survey Bulletine 2004, p. 19.

Cox, D.P. and Singer, D.A., eds., 1986, Mineral deposit models; U.S. Geological Survey Bulletin 1693, 379 p.

Doebrich, J. L., 1995, Geology and mineral deposits of the Antler Peak 7.5-minute quadrangle, Lander County, Nevada: Nevada Bureau of Mines and Geology Bulletin 109, map scale 1:24,000, 44 p.

Keeler, D. A., 2010, Structural reconstruction of the Copper Basin area, Battle Mountain district, Nevada: Unpublished M. S. thesis, Tucson, University of Arizona, 92 p.

Kizis, J. A., Jr., Bruff, S. R., Crist, E. M., Mough, D. C., and Vaughan, R. G., 1997, Empirical geologic modeling in intrusion-related gold exploration: An example from the Buffalo Valley area, northern Nevada: SEG Newsletter, no. 30, p. 1, 6-13.

McComb, 2009

McKee, E. H., 2000, Potassium-argon chronology of Cretaceous and Cenozoic igneous activity, hydrothermal alteration, and mineralization, *in* Theodore, T. G., ed., Geology of pluton-related gold mineralization at Battle Mountain, Nevada: Tucson, Arizona, Center for Mineral Resources, Monographs in Mineral Resource Science No. 2, p. 121-126.

Meinert, L. D., 2000, Gold in skarns related to epizonal intrusions, *in* Hagemann, S. G., and Brown, P. E., eds., Gold in 2000: Reviews in Economic Geology, v. 13, p. 347-375.

Meinert, L. D., Dipple, G. M., and Nicolescu, S., 2005, World skarn deposits, *in* Hedenquist, J. W., Thompson, J. F. H., Goldfarb, R. J., and Richards, J. P., eds., Economic Geology 100th Anniversary Volume, p. 299-336.

Murchey, B. L., 1989, Late Paleozoic siliceous basins of the western Cordillera of North America (Nevada, California, Mexico, and Alaska): Three studies using radiolarians and sponge spicules for stratigraphic, paleobathymetric, and tectonic analysis: Unpublished Ph. D. thesis, University of California, Santa Cruz, 189 p.

Murchey, B. L., 1990, Age and depositional setting of siliceous sediments in the upper Paleozoic Havallah sequence near Battle Mountain, Nevada; Implications for the paleogeography and structural evolution of the western margin of North America, *in* Harwood, D. S., and Miller, M. M., eds., Paleozoic and early Mesozoic paleogeographic relations; Sierra Nevada Klamath Mountains, and related terranes: Geological Society of America Special Paper 255, p. 137-155.

Reid, R. F., Nicholes, J., Kofoed, R., McComb, M., and Sechrist, K. J., 2011, Buffalo Valley gold mine: Porphyry copper, gold skarn or distal disseminated precious-metal deposit, *in* Steininger, R. C., and Pennell, W. M., eds., Great Basin evolution and metallogeny, Geological Society of Nevada, Symposium, Reno/Sparks, May 2010, Proceedings, v. 2, p. 637-656.

Roberts, R. J., 1964, Stratigraphy and structure of the Antler Peak quadrangle, Humboldt and Lander Counties, Nevada: U. S. Geological Survey Professional Paper 459-A, 93 p.

Roberts, R. J., and Arnold, D. C., 1965, Ore deposits of the Antler Peak quadrangle, Humboldt and Lander Counties, Nevada: U. S. Geological Survey Professional Paper 459-B, 94 p.

Seedorff, E., Bailey, C. R. G., Kelley, D., and Parks, W., 1991, Buffalo Valley mine: A porphyry-related gold deposit, Lander County, Nevada, *in* Buffa, R., and Coyner, A. R., eds., Field Trip Guidebook Compendium, Geology and ore deposits of the Great Basin, Geological Society of Nevada, Symposium, Reno/Sparks, April 1990, Proceedings, v. 2, p. 969-987.

Stewart, J. H., MacMillan, J. R., Nichols, K. M., and Stevens, C. H., 1977, Deep-water upper Paleozoic rocks in north-central Nevada--A study of the type-area of the Havallah Formation, *in* Stewart, J. H., Stevens, C. H., and Fritsche, A. E., eds., Paleozoic paleogeography of the western United States, Pacific Coast Paleogeography Symposium 1, Society of Economic Paleontologists and Mineralogists, Pacific Section, p. 337-347.

Stewart, J. H., Murchey, B., Jones, D. L., and Wardlaw, B. R., 1986, Paleontologic evidence for complex tectonic interlayering of Mississippian to Permian deep-water rocks of the Golconda allochthon in Tobin Range, north-central Nevada: Geological Society of America Bulletin, v. 97, p. 1122-1132.

Theodore, T. G., 2000, Geology of pluton-related gold mineralization at Battle Mountain, Nevada, *with sections by* E. H. McKee, E. I. Bloomstein, B. L. Braginton, R. W. Owen, R. L. Parratt, K. C. Raabe, W. F. Thompson, D. H. McGibbon, A. B. Wallace, R. P. Felder, R. L. Oscarson, and D. M. DeR. Channer: Tucson, Arizona, Center for Mineral Resources, Monographs in Mineral Resource Science No. 2, scale of maps 1:24,000, 271 p.

Theodore, T. G., Silberman, M. L., and Blake, D. W., 1973, Geochemistry and potassium-argon ages of plutonic rocks in the Battle Mountain mining district, Lander County, Nevada: U. S. Geological Survey Professional Paper 798-A, 24 p.

Tingley, J. V., 1992, Mining districts of Nevada: Nevada Bureau of Mines and Geology Report 47, 124 p.

Tomlinson, A. J., 1990, Biostratigraphy, stratigraphy, sedimentary petrology, and structural geology of the upper Paleozoic Golconda allochthon, north-central Nevada: Unpublished Ph. D. thesis, Stanford California, Stanford University, 491 p.

Williams, H., Turner, F. J., and Gilbert, C. M., 1982, Petrography: An introduction to the study of rocks in thin section, 2nd Edition: San Francisco, W. H. Freeman and Company, 626 p.

Figures

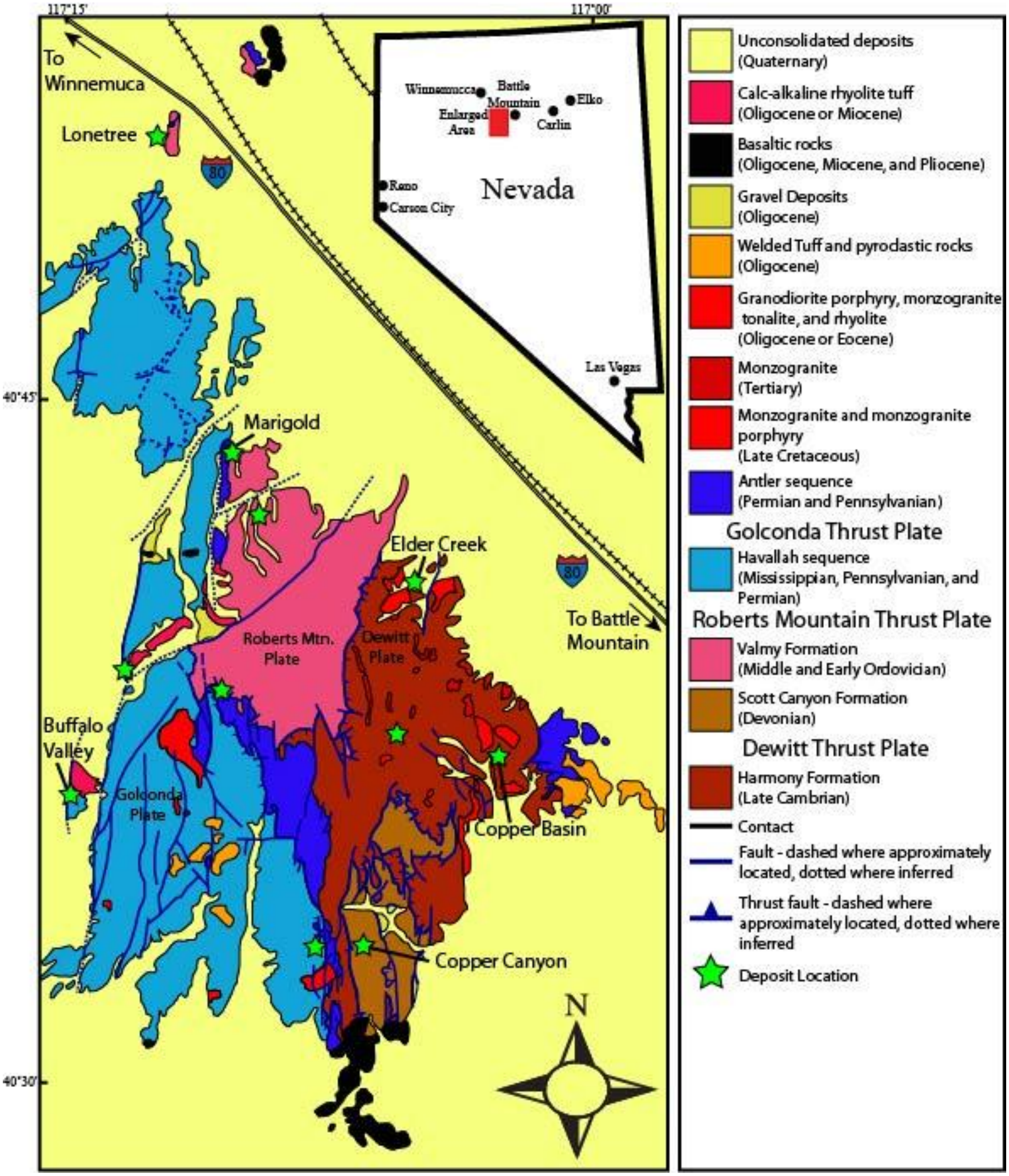

Figure 1. Generalized geology of Battle Mountain, Nevada showing the distinct thrust plates that constitute the major part of the range as well as deposits in the district. (modified from Theodore, 2000).

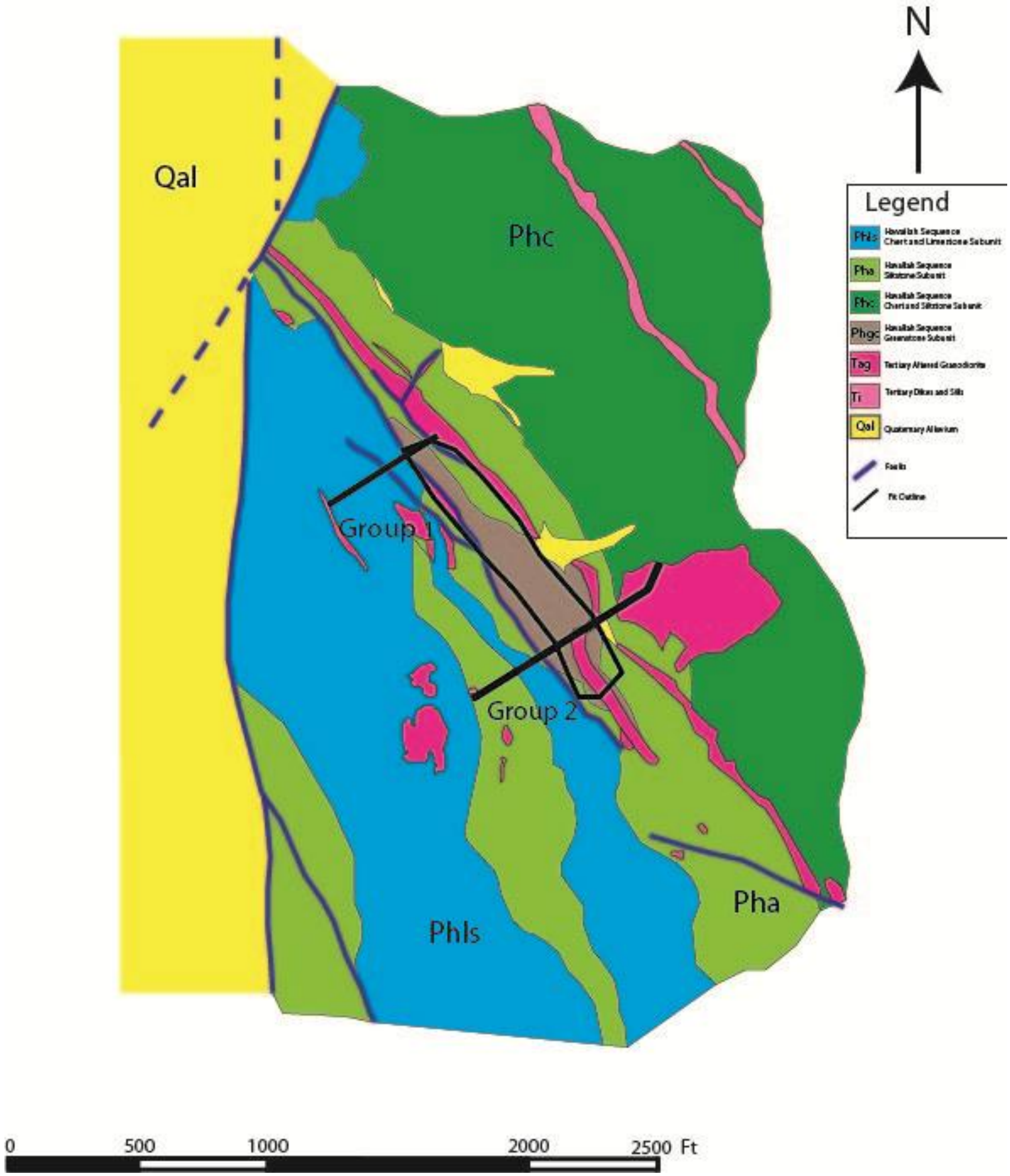

Figure 2. General geologic map of Buffalo Valley. (Modified from Reid et al., 2011).

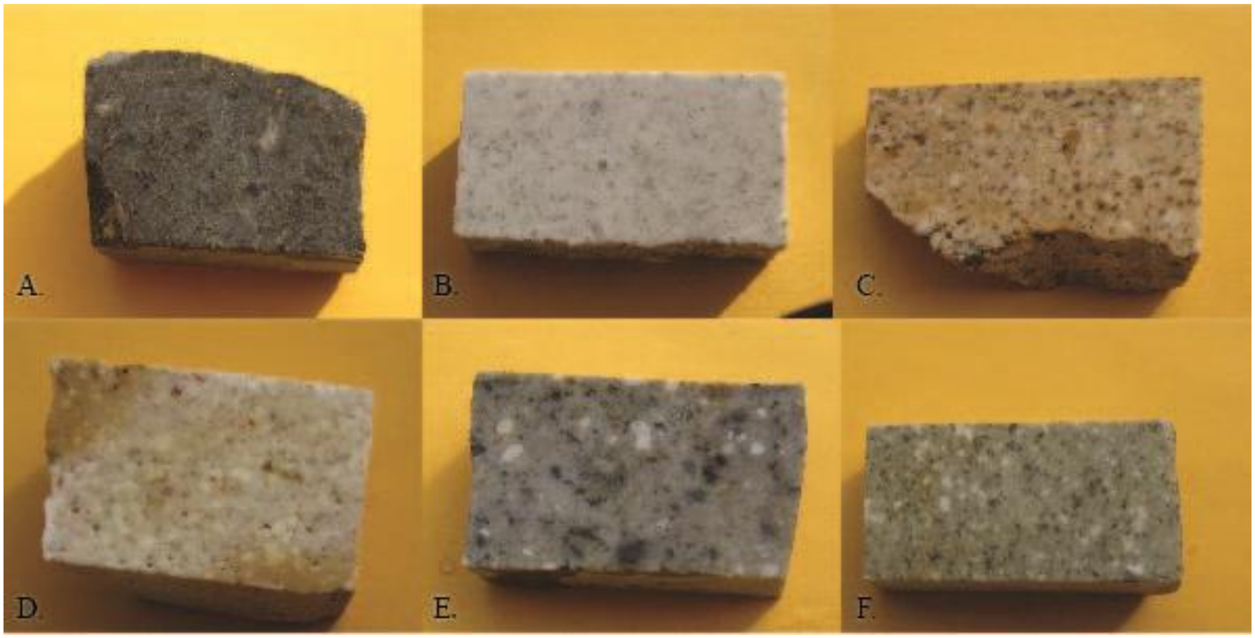

Figure 3. Various igneous rocks at Buffalo Valley. A is the greenstone (Phgc) and the B-F are granodiorite.

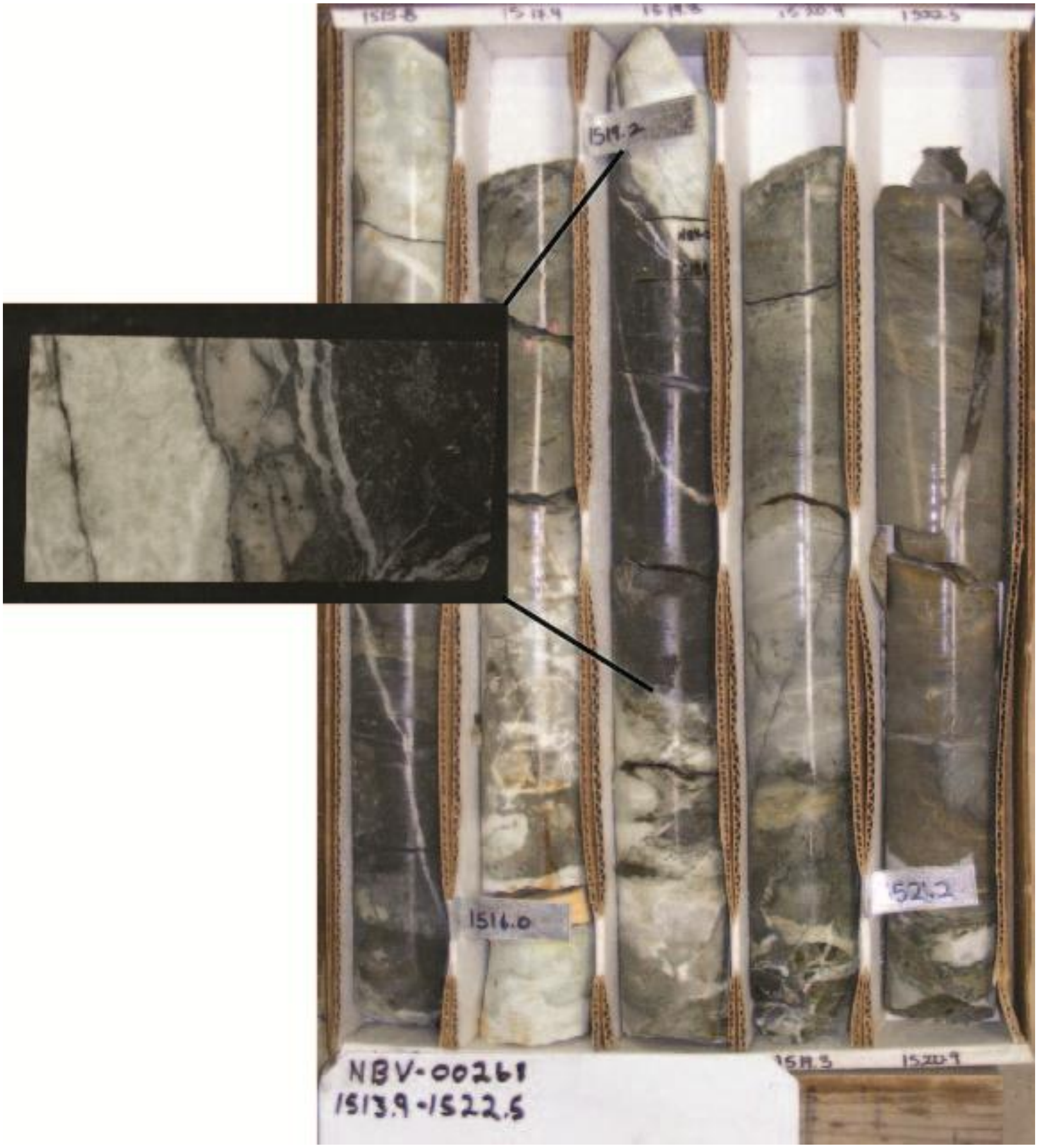

Figure 4. Dark, fine grained “mystery rock” intruding into a white diopside-wollastonite skarn material. Ghosts of phenocrysts can be discerned in the insert of the billet.

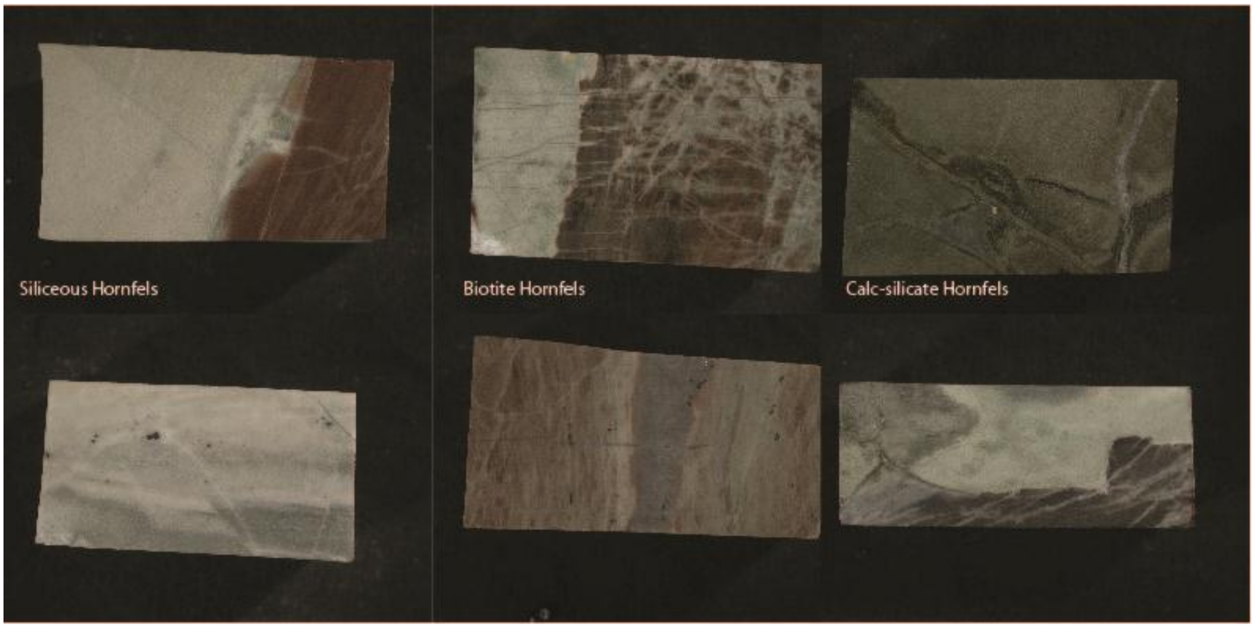

Figure 5. Various hornfels within the Havallah Sequence. Note the wispy textures within the biotite hornfelsed material.

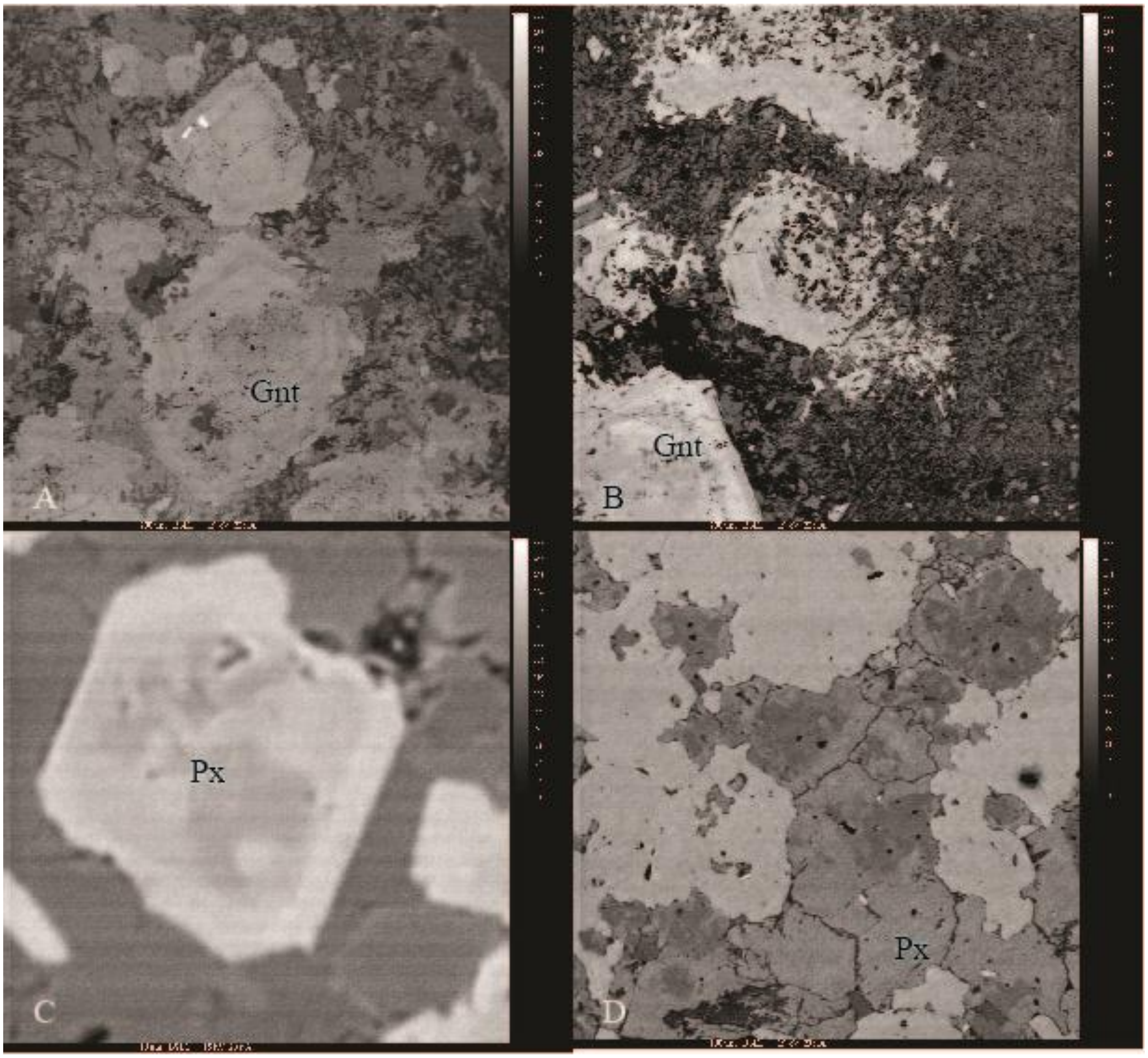

Figure 6. Zoned garnets and pyroxenes from skarn altered calcareous units within the Havallah sequence.

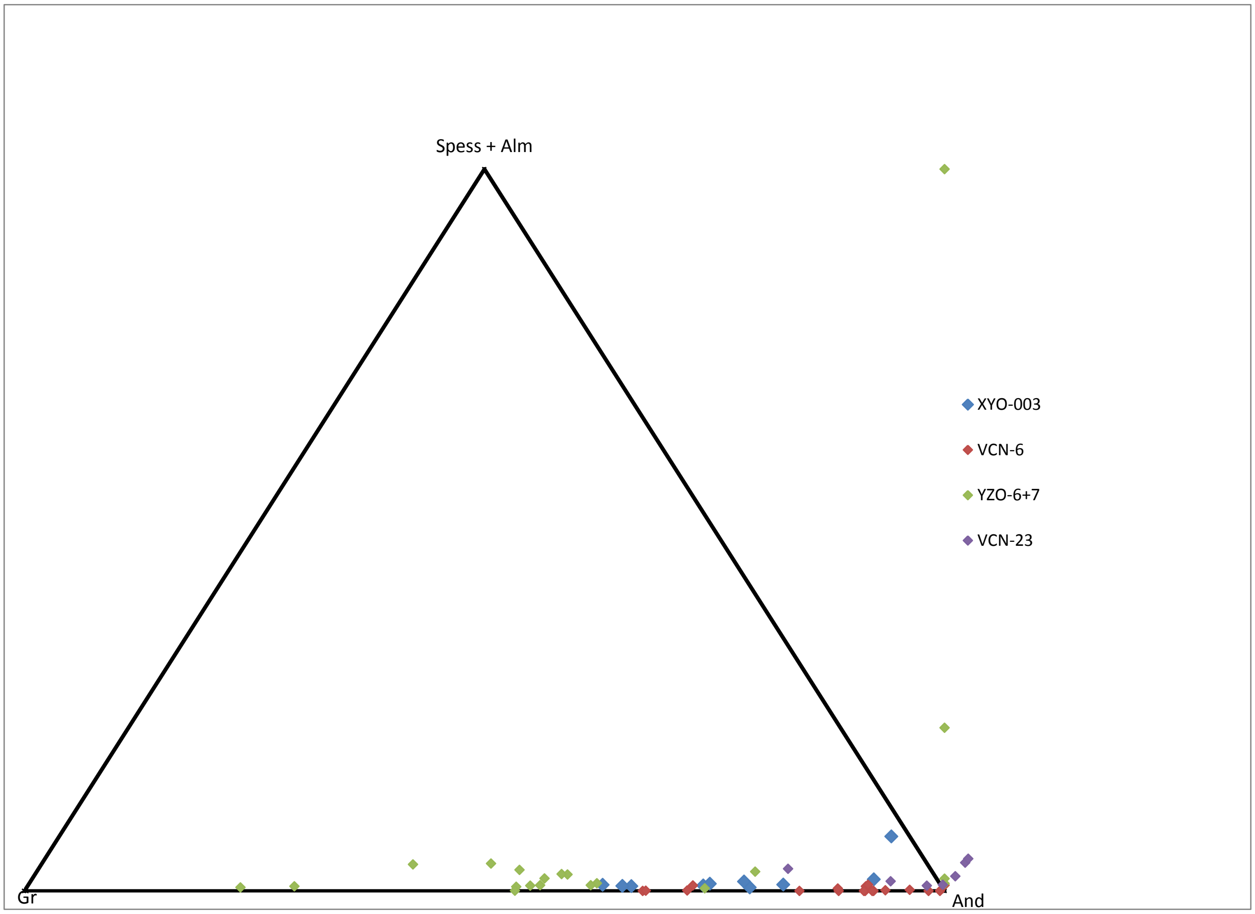

Figure 7. Ternary plot showing garnet compositions in skarned Havallah sequence limestone by sample.

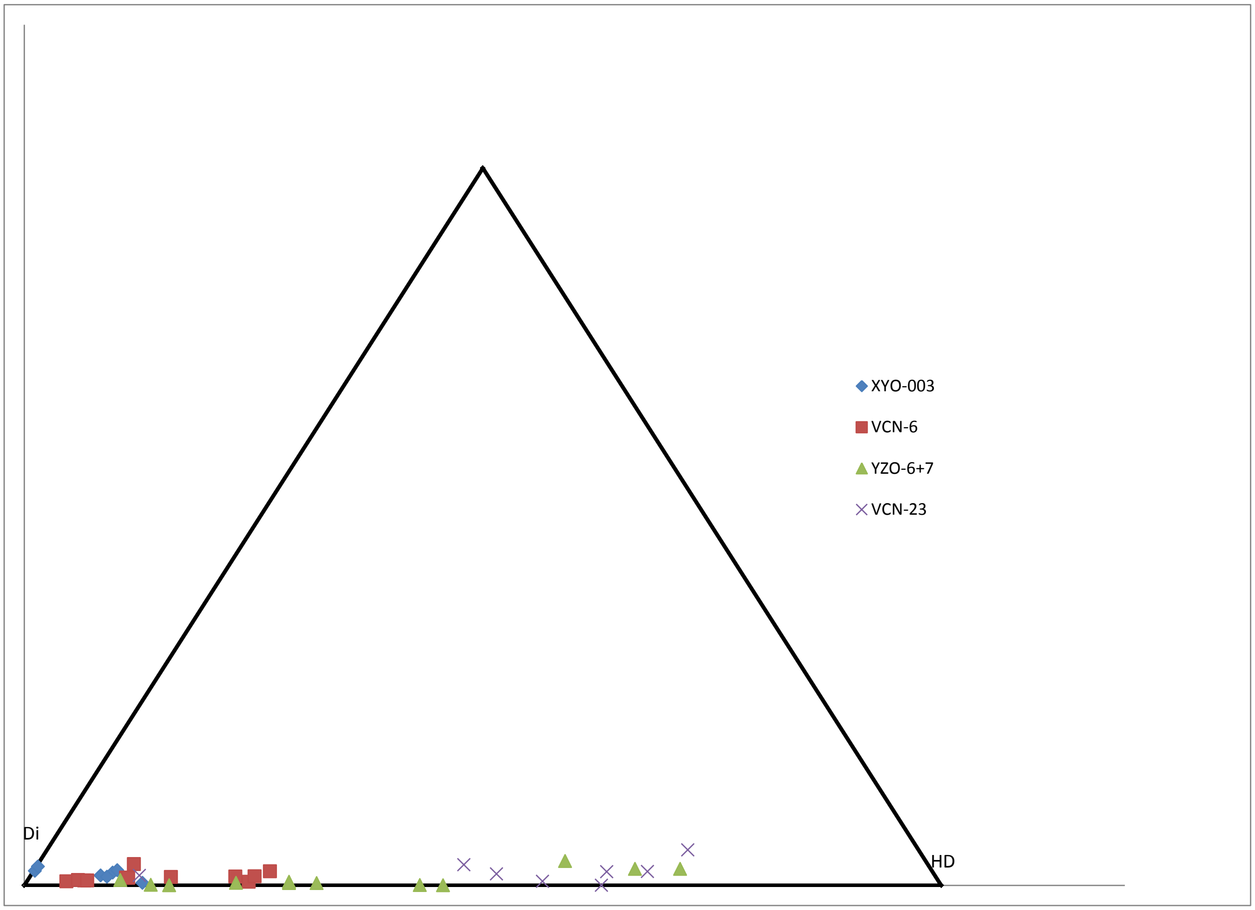

Figure 8. Ternary plot showing pyroxene compositions in skarned Havallah sequence limestone by sample.

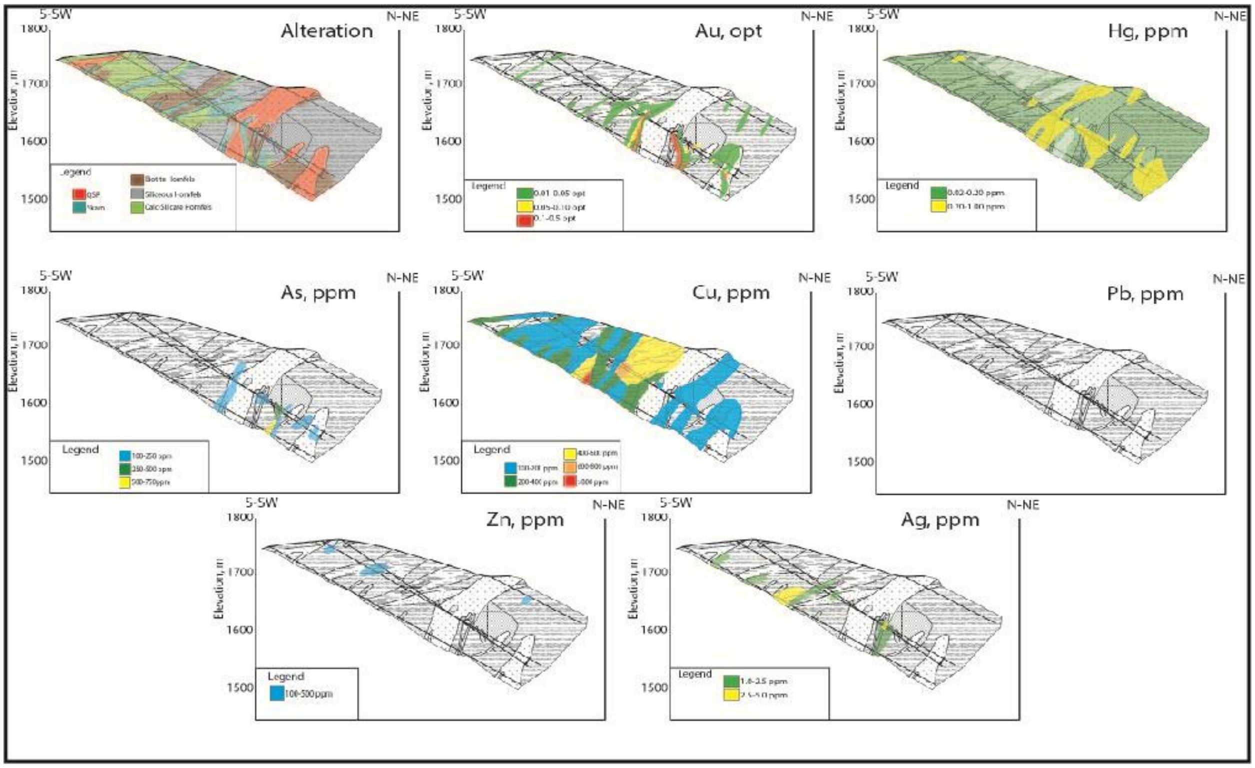

Figure 9. Cross section group 1 showing overlays of alteration, Au, Hg, As, Cu, Pb, Zn and Ag over lithology.

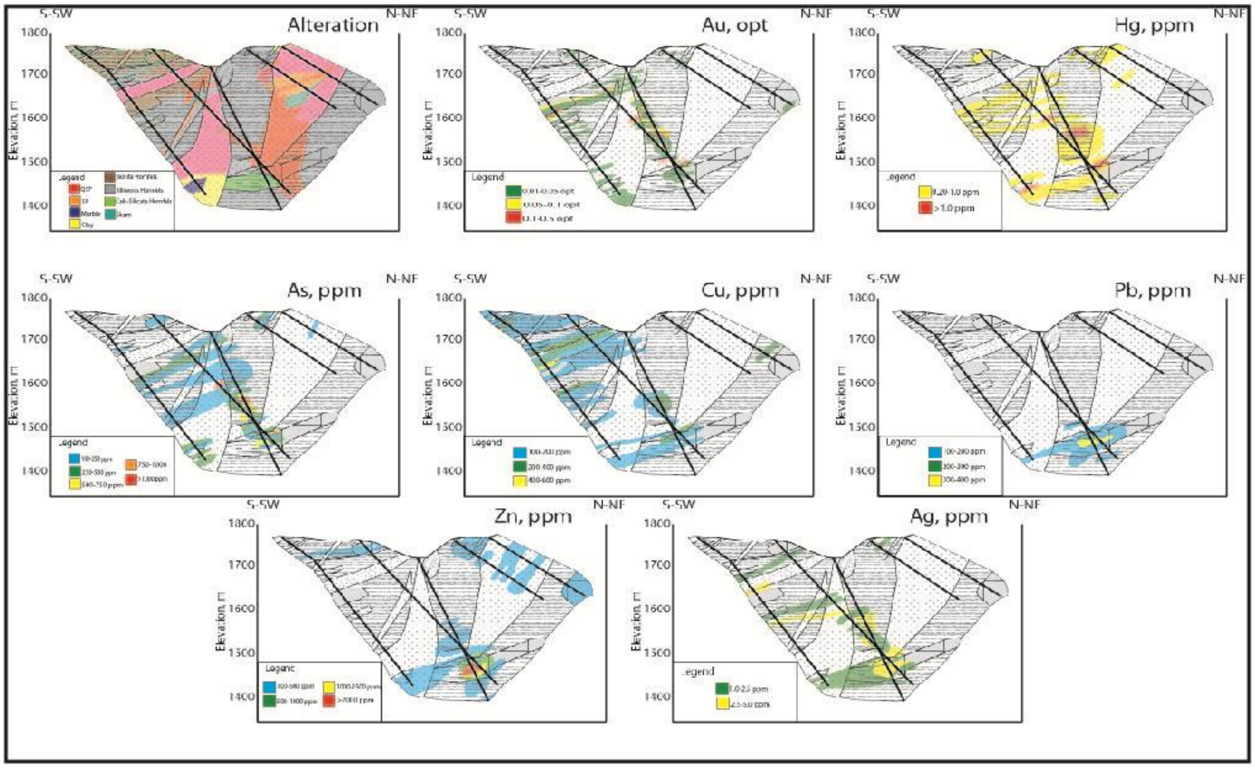

Figure 10. Cross sections from Group 2 showing over;ays of alteration, Au, Hg, As, Cu, Pb, Zn and Ag.

Tables

Analyses of Igneous Rocks at Buffalo Valley					
	1	2	3	4	5
SiO2	61.90	63.80	69.20	65.60	69.40
Al_2O_3	16.30	16.30	15.20	15.90	15.20
FeO_3	2.05	0.55	0.62	3.32	0.89
FeO	3.00	1.29	0.99	0.92	1.08
MgO	1.88	1.85	1.09	1.61	1.12
CaO	4.86	8.49	1.71	3.55	1.05
Na_2O	3.11	2.54	4.64	2.38	5.55
K_2O	2.30	1.97	2.92	2.51	2.63
TiO_2	0.55	0.57	0.25	0.53	0.26
P_2O_5	0.24	0.25	0.10	0.23	0.10
MnO	0.10	0.05	0.03	0.04	0.06
H_2O+	1.80	1.03	1.24	1.60	1.11
H_2O-	0.45	0.39	0.32	1.04	0.25
CO_2	0.92	0.36	0.80	0.01 L	0.38
Total	99.46	99.44	100.37	99.24	99.08

Table 1. Chemical analyses in weight percent by wavelength dispersive X-ray spectroscopy (modified from Doebrich, 1995). L-below lower detection limit shown. 1 is from the granodiorite porphyry stock , east of the Buffalo Valley open-pit. 2 is from a granodiorite porphyry plug , southwest of the Buffalo Valley open-pit. 3 is from the a granodiorite porphyry dike in the center of the Buffalo Valley open-pit. 4 is from the granodiorite porphyry dike at the southwest end of the Buffalo Valley open-pit. 5 is from the large continuous northwest-trending dike, southeast Buffalo Valley.

Arsenopyrite (FeAsS)

	1	2	3
		XKB-25	
Cr	0.000	0.000	0.000
Mn	0.000	0.000	0.000
Fe	1.002	0.988	0.978
Co	0.000	0.003	0.017
Ni	0.000	0.002	0.009
Cu	0.000	0.001	0.001
Zn	0.000	0.000	0.000
As	1.018	0.974	0.927
Ag	0.000	0.000	0.000
Sb	0.013	0.011	0.011
Te	0.000	0.001	0.001
Au	0.000	0.000	0.000
Pb	0.000	0.000	0.000
Bi	0.002	0.000	0.001
Σ	2.035	1.981	1.945
S Site Filling			
S	0.965	1.019	1.055
Σ	0.965	1.019	1.055
Total Sites in Formula			
Σ+S	3.000	3.000	3.000

Normalized electron microprobe data and site fillings for arsenopyrite calculated based on the total number of site fillings in the mineral formula.

Pyrite (FeS_2)

	1	2	3	4	5	6	7	8	9	10	11	12	13	14	15	16	17
									XKB-6								
Cr	0.000	0.000	0.000	0.000	0.000	0.000	0.000	0.000	0.000	0.000	0.000	0.000	0.000	0.000	0.000	0.000	0.000
Mn	0.000	0.000	0.000	0.000	0.000	0.000	0.000	0.000	0.000	0.000	0.000	0.000	0.000	0.000	0.000	0.000	0.000
Fe	0.995	0.993	0.996	0.997	0.983	0.994	0.996	0.988	0.993	0.982	0.952	0.998	0.981	1.001	0.999	0.996	0.998
Co	0.000	0.000	0.000	0.000	0.001	0.000	0.000	0.000	0.000	0.000	0.003	0.000	0.000	0.000	0.000	0.000	0.000
Ni	0.000	0.001	0.000	0.000	0.008	0.000	0.000	0.002	0.001	0.004	0.035	0.002	0.016	0.000	0.000	0.000	0.000
Cu	0.000	0.000	0.000	0.000	0.000	0.000	0.000	0.000	0.000	0.000	0.000	0.000	0.000	0.000	0.000	0.000	0.000
Zn	0.000	0.000	0.000	0.000	0.000	0.000	0.000	0.000	0.000	0.000	0.000	0.000	0.000	0.000	0.000	0.000	0.000
As	0.000	0.000	0.000	0.000	0.000	0.000	0.001	0.000	0.000	0.009	0.000	0.000	0.000	0.000	0.000	0.000	0.000
Ag	0.000	0.000	0.000	0.000	0.000	0.000	0.000	0.000	0.000	0.000	0.000	0.000	0.000	0.000	0.000	0.000	0.000
Sb	0.000	0.000	0.000	0.001	0.001	0.000	0.000	0.000	0.000	0.000	0.000	0.000	0.000	0.001	0.000	0.000	0.000
Te	0.000	0.000	0.000	0.000	0.000	0.000	0.000	0.000	0.000	0.000	0.000	0.000	0.000	0.000	0.000	0.000	0.000
Au	0.000	0.000	0.000	0.000	0.000	0.000	0.000	0.000	0.000	0.000	0.000	0.000	0.000	0.000	0.000	0.000	0.000
Pb	0.000	0.000	0.000	0.000	0.000	0.000	0.000	0.000	0.000	0.000	0.000	0.000	0.000	0.000	0.000	0.000	0.000
Bi	0.000	0.000	0.000	0.000	0.000	0.000	0.000	0.000	0.000	0.000	0.000	0.000	0.000	0.000	0.000	0.000	0.000
Σ	0.996	0.995	0.997	1.000	0.994	0.995	0.997	0.990	0.994	0.997	0.990	1.001	0.998	1.004	0.999	0.996	0.998
S Site Filling																	
S	2.004	2.005	2.003	2.000	2.006	2.005	2.003	2.010	2.006	2.003	2.010	1.999	2.002	1.996	2.001	2.004	2.002
Σ	2.004	2.005	2.003	2.000	2.006	2.005	2.003	2.010	2.006	2.003	2.010	1.999	2.002	1.996	2.001	2.004	2.002
Total Sites in Formula																	
Σ+S	3.000	3.000	3.000	3.000	3.000	3.000	3.000	3.000	3.000	3.000	3.000	3.000	3.000	3.000	3.000	3.000	3.000

	18	19	20	21	22	23	24	25	26
			XKB-5				XKB-25		XKB-63
Cr	0.000	0.000	0.000	0.000	0.000	0.000	0.000	0.000	0.000
Mn	0.000	0.000	0.000	0.000	0.000	0.000	0.001	0.000	0.000
Fe	0.963	0.987	0.996	0.990	0.992	0.989	0.989	0.990	1.009
Co	0.000	0.000	0.000	0.000	0.000	0.001	0.000	0.000	0.000
Ni	0.000	0.000	0.000	0.000	0.000	0.000	0.000	0.003	0.001
Cu	0.001	0.001	0.000	0.000	0.000	0.000	0.000	0.000	0.000
Zn	0.002	0.003	0.000	0.000	0.000	0.001	0.000	0.000	0.000
As	0.175	0.069	0.003	0.008	0.003	0.011	0.000	0.000	0.000
Ag	0.000	0.000	0.000	0.000	0.000	0.000	0.000	0.000	0.000
Sb	0.002	0.002	0.000	0.000	0.000	0.000	0.000	0.000	0.000
Te	0.000	0.000	0.000	0.000	0.000	0.000	0.000	0.000	0.000
Au	0.000	0.000	0.000	0.000	0.000	0.000	0.000	0.000	0.000
Pb	0.000	0.000	0.000	0.000	0.000	0.000	0.000	0.000	0.000
Bi	0.000	0.000	0.000	0.000	0.000	0.000	0.000	0.000	0.000
Σ	1.144	1.061	1.000	0.999	0.996	1.003	0.991	0.993	1.010
S Site Filling									
S	1.856	1.939	2.000	2.001	2.004	1.997	2.009	2.007	1.990
Σ	1.856	1.939	2.000	2.001	2.004	1.997	2.009	2.007	1.990
Total Sites in Formula									
Σ+S	3.000	3.000	3.000	3.000	3.000	3.000	3.000	3.000	3.000

Normalized electron microprobe data, site fillings for pyrite. Pyrite is calculated on the total number of sites in the mineral formula.

Table 4. Normalized electron microprobe data and site fillings for arsenopyrite and pyrite.

Arsenopyrite (FeAsS)			
	1	2	3
	XKB-25		
Cr	0.00	0.00	0.00
Mn	0.00	0.00	0.00
Fe	33.95	34.05	33.92
Co	0.01	0.12	0.61
Ni	0.00	0.08	0.32
Cu	0.00	0.04	0.02
Zn	0.00	0.00	0.00
As	46.25	45.01	43.13
Ag	0.00	0.00	0.00
Sb	0.98	0.85	0.85
Te	0.01	0.05	0.07
Au	0.00	0.03	0.01
Pb	0.00	0.00	0.00
Bi	0.20	0.05	0.08
S	18.77	20.16	21.01
Total	100.17	100.44	100.02

Appendix Table 2. Raw weight % electron microprobe data for arsenopyrite

Pyrite (FeS_2)																										
	1	2	3	4	5	6	7	8	9	10	11	12	13	14	15	16	17	18	19	20	21	22	23	24	25	26
	XKB-6																	XKB-5						XKB-25		XKB-63
Cr	0.01	0.01	0.01	0.01	0.01	0.01	0.01	0.01	0.01	0.01	0.00	0.00	0.00	0.01	0.00	0.00	0.00	0.02	0.01	0.00	0.00	0.00	0.00	0.00	0.00	0.00
Mn	0.00	0.00	0.00	0.00	0.00	0.00	0.00	0.01	0.01	0.00	0.00	0.00	0.00	0.00	0.00	0.00	0.00	0.00	0.00	0.01	0.01	0.01	0.02	0.04	0.00	0.00
Fe	45.99	45.68	46.06	45.66	45.30	46.03	45.96	45.29	45.42	45.32	44.05	46.42	45.55	46.14	46.18	46.21	46.33	42.35	44.54	45.83	45.68	45.76	45.17	45.75	45.87	46.07
Co	0.00	0.01	0.00	0.00	0.07	0.00	0.00	0.01	0.00	0.01	0.15	0.00	0.02	0.00	0.00	0.00	0.00	0.02	0.01	0.02	0.01	0.01	0.03	0.00	0.00	0.01
Ni	0.00	0.04	0.00	0.01	0.41	0.00	0.01	0.10	0.03	0.19	1.72	0.12	0.77	0.02	0.00	0.00	0.00	0.00	0.00	0.01	0.00	0.00	0.01	0.00	0.14	0.03
Cu	0.00	0.00	0.00	0.00	0.00	0.00	0.00	0.00	0.00	0.01	0.00	0.00	0.01	0.00	0.00	0.00	0.00	0.04	0.03	0.00	0.00	0.00	0.00	0.00	0.01	0.02
Zn	0.00	0.00	0.00	0.01	0.00	0.01	0.01	0.00	0.01	0.00	0.00	0.00	0.00	0.02	0.01	0.01	0.00	0.12	0.15	0.00	0.01	0.00	0.08	0.00	0.00	0.00
As	0.00	0.01	0.00	0.02	0.00	0.01	0.05	0.00	0.01	0.58	0.00	0.00	0.00	0.00	0.00	0.00	0.00	10.30	4.15	0.17	0.47	0.21	0.68	0.00	0.00	0.00
Ag	0.01	0.00	0.00	0.00	0.00	0.00	0.01	0.00	0.00	0.01	0.00	0.01	0.00	0.00	0.01	0.00	0.00	0.02	0.02	0.01	0.00	0.00	0.00	0.01	0.01	0.01
Sb	0.00	0.01	0.05	0.14	0.09	0.01	0.00	0.00	0.01	0.03	0.00	0.01	0.00	0.13	0.01	0.00	0.01	0.22	0.19	0.04	0.04	0.02	0.02	0.00	0.00	0.00
Te	0.00	0.00	0.00	0.00	0.00	0.00	0.00	0.00	0.00	0.00	0.00	0.00	0.00	0.00	0.00	0.00	0.00	0.00	0.00	0.00	0.00	0.00	0.00	0.00	0.00	0.00
Au	0.00	0.00	0.00	0.00	0.00	0.00	0.00	0.00	0.00	0.00	0.00	0.00	0.00	0.00	0.00	0.00	0.00	0.00	0.00	0.00	0.00	0.00	0.00	0.00	0.00	0.01
Pb	0.00	0.00	0.00	0.00	0.00	0.00	0.00	0.00	0.00	0.00	0.00	0.00	0.00	0.00	0.00	0.00	0.00	0.00	0.00	0.00	0.00	0.00	0.00	0.00	0.00	0.00
Bi	0.00	0.00	0.00	0.00	0.00	0.00	0.00	0.00	0.02	0.00	0.01	0.00	0.01	0.03	0.01	0.00	0.00	0.00	0.00	0.00	0.00	0.00	0.02	0.04	0.00	0.00
S	53.17	52.97	53.20	52.58	53.09	53.32	53.07	52.91	52.69	53.07	53.42	53.36	53.38	52.81	53.13	53.39	53.38	46.89	50.24	52.82	53.01	53.07	52.37	53.35	53.42	52.19
Total	99.18	98.73	99.32	98.43	98.97	99.39	99.12	98.33	98.21	99.23	99.35	99.92	99.74	99.16	99.35	99.61	99.72	99.98	99.34	98.91	99.23	99.08	98.40	99.19	99.45	98.34

Appendix Table 1. Raw weight % electron microprobe data for pyrites.

	1	2	3	4	5	6	7	8	9	10	11	12	13	14	15	16	17
Oxides																	
	XYO-003			VCN-6				YZO-7		YZO-6		VCN-23		XYO-003		VCN-6	
SiO_2	54.74	54.70	54.96	55.26	55.38	54.64	54.59	55.34	53.42	53.86	52.82	52.00	51.45	54.81	54.59	51.04	53.72
TiO_2	0.02	0.02	0.03	0.02	0.02	0.00	0.00	0.03	0.10	0.05	0.07	0.02	0.03	0.03	0.10	0.03	0.00
Al_2O_3	0.68	0.66	0.62	0.25	0.17	0.17	0.17	0.00	0.60	0.76	0.42	0.19	0.25	0.87	1.06	0.72	0.30
Cr_2O_3	0.01	0.03	0.01	0.00	0.01	0.00	0.04	0.00	0.18	0.03	0.03	0.05	0.01	0.04	0.03	0.00	0.00
V_2O_3	0.00	0.00	0.00	0.00	0.00	0.00	0.00	0.00	0.13	0.00	0.04	0.03	0.00	0.01	0.00	0.00	0.04
Fe_2O_3	0.00	0.00	0.00	0.00	0.00	0.00	0.00	0.00	0.00	0.00	0.00	0.64	0.00	0.00	0.00	2.08	0.00
FeO	2.37	2.66	2.65	1.36	1.72	3.43	2.06	3.24	7.02	4.34	8.80	13.71	16.88	2.78	4.05	6.81	7.60
MnO	0.56	0.65	0.68	0.21	0.27	0.39	0.25	0.27	0.26	0.26	0.23	1.02	0.66	0.76	0.80	0.61	0.48
MgO	16.35	15.95	16.41	17.20	16.88	16.08	16.70	16.33	13.35	15.31	12.33	8.97	7.42	15.95	15.70	11.11	13.43
CaO	25.58	25.53	25.43	25.75	25.64	25.41	25.58	25.54	24.64	25.01	24.46	24.17	23.19	25.95	25.19	26.24	24.73
ZnO	0.10	0.00	0.00	0.09	0.05	0.00	0.04	0.00	0.00	0.04	0.07	0.09	0.00	0.07	0.15	0.04	0.00
Na_2O	0.03	0.04	0.05	0.00	0.01	0.01	0.00	0.01	0.12	0.05	0.07	0.16	0.07	0.03	0.08	0.08	0.01
K_2O	0.01	0.01	0.01	0.00	0.00	0.00	0.01	0.00	0.00	0.01	0.01	0.00	0.00	0.00	0.01	0.00	0.00
F	0.17	0.15	0.05	0.03	0.00	0.00	0.00	0.00	0.18	0.05	0.00	0.00	0.00	0.08	0.00	0.00	0.06
Cl	0.00	0.00	0.00	0.00	0.00	0.00	0.00	0.00	0.00	0.00	0.00	0.00	0.00	0.00	0.00	0.00	0.00
Total	100.61	100.39	100.92	100.15	100.16	100.14	99.43	100.77	100.01	99.77	99.35	101.04	99.95	101.38	101.76	98.76	100.38
T Sites																	
Si	2.00	2.00	1.99	2.00	2.00	2.00	2.00	2.00	2.00	1.99	2.00	1.99	2.00	1.99	1.98	1.95	2.00
Al^{+3}	0.00	0.00	0.01	0.00	0.00	0.00	0.00	0.00	0.00	0.01	0.00	0.01	0.00	0.01	0.02	0.03	0.00
Fe^{+3}	0.00	0.00	0.00	0.00	0.00	0.00	0.00	0.00	0.00	0.00	0.00	0.00	0.00	0.00	0.00	0.01	0.00
T Sites Total	2.00	2.00	2.00	2.00	2.00	2.00	2.00	2.00	2.00	2.00	2.00	2.00	2.00	2.00	2.00	2.00	2.00
M1 Sites																	
Al	0.02	0.03	0.02	0.01	0.01	0.01	0.01	0.00	0.02	0.02	0.02	0.00	0.01	0.02	0.02	0.00	0.01
Fe^{+3}	0.00	0.00	0.00	0.00	0.00	0.00	0.00	0.00	0.00	0.00	0.00	0.02	0.00	0.00	0.00	0.05	0.00
Ti^{+4}	0.00	0.00	0.00	0.00	0.00	0.00	0.00	0.00	0.00	0.00	0.00	0.00	0.00	0.00	0.00	0.00	0.00
Cr	0.00	0.00	0.00	0.00	0.00	0.00	0.00	0.00	0.01	0.00	0.00	0.00	0.00	0.00	0.00	0.00	0.00
V	0.00	0.00	0.00	0.00	0.00	0.00	0.00	0.00	0.00	0.00	0.00	0.00	0.00	0.00	0.00	0.00	0.00
Zn	0.00	0.00	0.00	0.00	0.00	0.00	0.00	0.00	0.00	0.00	0.00	0.00	0.00	0.00	0.00	0.00	0.00
Mg	0.88	0.87	0.88	0.93	0.91	0.87	0.91	0.88	0.74	0.84	0.69	0.51	0.43	0.86	0.84	0.63	0.74
Fe^{+2}	0.07	0.08	0.08	0.04	0.05	0.11	0.06	0.10	0.22	0.13	0.28	0.44	0.55	0.08	0.12	0.22	0.24
Mn	0.02	0.02	0.01	0.01	0.01	0.01	0.01	0.01	0.00	0.00	0.00	0.03	0.01	0.02	0.00	0.02	0.01
M1 Sites Total	1.00	1.00	1.00	0.99	0.98	1.00	0.99	0.99	1.00	1.00	1.00	1.00	1.00	0.99	1.00	0.92	1.00
M2 Sites																	
Mg	0.00	0.00	0.00	0.00	0.00	0.00	0.00	0.00	0.00	0.00	0.00	0.00	0.00	0.00	0.00	0.00	0.00
Fe^{+2}	0.00	0.00	0.00	0.00	0.00	0.00	0.00	0.00	0.00	0.00	0.00	0.00	0.00	0.00	0.00	0.00	0.00
Mn	0.00	0.00	0.01	0.00	0.00	0.00	0.00	0.00	0.00	0.01	0.00	0.00	0.02	0.00	0.02	0.00	0.01
Ca	1.00	1.00	0.99	1.00	1.00	1.00	1.00	1.00	0.99	0.99	0.99	0.99	0.97	1.00	0.98	1.00	0.99
Na	0.00	0.00	0.00	0.00	0.00	0.00	0.00	0.00	0.01	0.00	0.00	0.01	0.01	0.00	0.00	0.00	0.00
M2 Sites Total	1.00	1.00	1.00	1.00	1.00	1.00	1.00	1.00	1.00	1.00	1.00	1.00	0.99	1.00	1.00	1.00	1.00

	18	19	20	21	22	23	24	25	26	27	28	29	30	31	32	33	34
Oxides																	
	VCN-6		YZO-7	YZO-6		VCN-23		VCN-6				YZO-7		YZO-6	VCN-23		
SiO_2	53.54	51.88	51.38	51.02	49.31	51.00	50.63	54.55	54.14	55.28	53.65	53.05	52.77	52.26	50.27	53.39	51.83
TiO_2	0.02	0.02	0.02	0.00	0.05	0.02	0.02	0.00	0.00	0.00	0.08	0.03	0.05	0.27	0.03	0.03	0.00
Al_2O_3	0.49	0.49	0.60	0.28	0.70	0.13	0.02	0.23	0.32	0.23	1.23	0.81	1.08	2.80	0.28	0.26	0.02
Cr_2O_3	0.01	0.00	0.04	0.03	0.04	0.00	0.00	0.04	0.03	0.00	0.00	0.27	0.18	0.12	0.00	0.01	0.05
V_2O_3	0.00	0.07	0.07	0.00	0.00	0.00	0.03	0.00	0.00	0.06	0.00	0.06	0.14	0.00	0.00	0.03	0.03
Fe_2O_3	0.00	0.89	0.00	0.55	0.42	0.50	0.00	0.00	0.00	0.00	0.00	0.00	0.00	0.13	1.07	0.00	0.00
FeO	3.10	7.22	18.62	16.46	20.04	18.37	19.61	4.86	3.29	1.96	6.84	8.53	9.44	4.82	19.30	19.98	15.33
MnO	1.72	0.43	0.81	1.24	0.79	0.80	2.09	0.56	0.39	0.25	0.48	0.17	0.22	0.12	0.89	0.65	0.75
MgO	15.30	12.60	5.58	7.00	4.80	6.23	4.85	15.15	15.85	16.81	13.43	12.01	11.46	14.41	5.40	6.40	8.45
CaO	24.34	25.11	23.06	23.66	23.29	23.50	22.52	25.09	25.18	25.74	24.91	24.66	24.34	25.33	23.23	21.45	24.04
ZnO	0.06	0.09	0.14	0.04	0.07	0.05	0.07	0.00	0.00	0.00	0.05	0.12	0.00	0.16	0.07	0.02	0.05
Na_2O	0.11	0.01	0.11	0.13	0.07	0.16	0.18	0.04	0.04	0.01	0.20	0.12	0.15	0.01	0.19	0.26	0.04
K_2O	0.00	0.01	0.00	0.00	0.00	0.00	0.00	0.00	0.00	0.01	0.00	0.01	0.00	0.00	0.01	0.01	0.00
F	0.07	0.00	0.10	0.00	0.06	0.00	0.00	0.00	0.10	0.00	0.25	0.00	0.00	0.00	0.02	0.00	0.09
Cl	0.00	0.00	0.00	0.00	0.00	0.00	0.00	0.00	0.00	0.00	0.00	0.00	0.00	0.00	0.00	0.00	0.00
Total	98.76	98.80	100.54	100.42	99.63	100.76	100.01	100.51	99.34	100.34	101.13	99.86	99.84	100.43	100.77	102.50	100.69
T Sites																	
Si	2.00	1.97	2.00	1.99	1.97	1.99	2.00	2.00	2.00	2.00	1.98	2.00	2.00	1.92	1.98	2.00	2.00
Al^{+3}	0.00	0.02	0.00	0.01	0.03	0.01	0.00	0.00	0.00	0.00	0.02	0.00	0.00	0.08	0.01	0.00	0.00
Fe^{+3}	0.00	0.01	0.00	0.00	0.00	0.00	0.00	0.00	0.00	0.00	0.00	0.00	0.00	0.00	0.01	0.00	0.00
T Sites Total	2.00	2.00	2.00	2.00	2.00	2.00	2.00	2.00	2.00	2.00	2.00	2.00	2.00	2.00	2.00	2.00	2.00
M1 Sites																	
Al	0.02	0.00	0.03	0.00	0.00	0.00	0.00	0.01	0.01	0.01	0.04	0.04	0.04	0.05	0.00	0.01	0.00
Fe^{+3}	0.00	0.02	0.00	0.02	0.01	0.01	0.00	0.00	0.00	0.00	0.00	0.00	0.00	0.00	0.02	0.00	0.00
Ti^{+4}	0.00	0.00	0.00	0.00	0.00	0.00	0.00	0.00	0.00	0.00	0.00	0.00	0.00	0.01	0.00	0.00	0.00
Cr	0.00	0.00	0.00	0.00	0.00	0.00	0.00	0.00	0.00	0.00	0.00	0.01	0.01	0.00	0.00	0.00	0.00
V	0.00	0.00	0.00	0.00	0.00	0.00	0.00	0.00	0.00	0.00	0.00	0.00	0.00	0.00	0.00	0.00	0.00
Zn	0.00	0.00	0.00	0.00	0.00	0.00	0.00	0.00	0.00	0.00	0.00	0.00	0.00	0.00	0.00	0.00	0.00
Mg	0.85	0.71	0.33	0.40	0.28	0.36	0.29	0.83	0.87	0.91	0.74	0.67	0.64	0.79	0.32	0.37	0.48
Fe^{+2}	0.10	0.23	0.61	0.54	0.67	0.60	0.65	0.15	0.10	0.06	0.21	0.27	0.30	0.15	0.64	0.62	0.49
Mn	0.03	0.01	0.03	0.04	0.03	0.02	0.06	0.01	0.01	0.01	0.01	0.01	0.00	0.00	0.02	0.00	0.02
M1 Sites Total	1.00	0.98	1.00	1.00	1.00	1.00	1.00	1.00	1.00	0.99	1.00	1.00	1.00	1.00	1.00	1.00	1.00
M2 Sites																	
Mg	0.00	0.00	0.00	0.00	0.00	0.00	0.00	0.00	0.00	0.00	0.00	0.00	0.00	0.00	0.00	0.00	0.00
Fe^{+2}	0.00	0.00	0.00	0.00	0.00	0.00	0.00	0.00	0.00	0.00	0.00	0.00	0.00	0.00	0.00	0.02	0.00
Mn	0.02	0.00	0.00	0.00	0.00	0.01	0.01	0.00	0.00	0.00	0.00	0.00	0.00	0.00	0.01	0.02	0.01
Ca	0.97	1.00	0.97	0.99	1.00	0.98	0.96	0.99	1.00	1.00	0.99	1.00	0.99	1.00	0.98	0.88	0.99
Na	0.01	0.00	0.01	0.01	0.00	0.01	0.01	0.00	0.00	0.00	0.01	0.00	0.01	0.00	0.01	0.02	0.00
M2 Sites Total	1.00	1.00	0.98	1.00	1.00	1.00	0.99	0.99	1.00	1.00	1.00	1.00	1.00	1.00	1.00	0.95	1.00

Table 3. Normalized electron microprobe data, oxide weights and the number of atoms per formula calculated using the normalization routine $\Sigma(T+M1+M2)=4$ for pyroxene associated with skarn alteration of the Havallah formation. 1-13 are pyroxene cores, 14-24 are pyroxene rims, and 25-34 are unzoned pyroxenes.

Analyses of Igneous Rocks at Buffalo Valley					
	1	2	3	4	5
SiO2	61.90	63.80	69.20	65.60	69.40
Al_2O_3	16.30	16.30	15.20	15.90	15.20
FeO_3	2.05	0.55	0.62	3.32	0.89
FeO	3.00	1.29	0.99	0.92	1.08
MgO	1.88	1.85	1.09	1.61	1.12
CaO	4.86	8.49	1.71	3.55	1.05
Na_2O	3.11	2.54	4.64	2.38	5.55
K_2O	2.30	1.97	2.92	2.51	2.63
TiO_2	0.55	0.57	0.25	0.53	0.26
P_2O_5	0.24	0.25	0.10	0.23	0.10
MnO	0.10	0.05	0.03	0.04	0.06
H_2O+	1.80	1.03	1.24	1.60	1.11
H_2O-	0.45	0.39	0.32	1.04	0.25
CO_2	0.92	0.36	0.80	0.01 L	0.38
Total	99.46	99.44	100.37	99.24	99.08

Table 1. Chemical analyses in weight percent by wavelength dispersive X-ray spectroscopy (modified from Doebrich, 1995). L-below lower detection limit shown. 1 is from the granodiorite porphyry stock , east of the Buffalo Valley open-pit. 2 is from a granodiorite porphyry plug , southwest of the Buffalo Valley open-pit. 3 is from the a granodiorite porphyry dike in the center of the Buffalo Valley open-pit. 4 is from the granodiorite porphyry dike at the southwest end of the Buffalo Valley open-pit. 5 is from the large continuous northwest-trending dike, southeast Buffalo Valley.